

EXPLORATION FOR POROSITY IN CARBONATES: A SYNTHETIC-BASED STUDY¹

DONNA FRASER² AND SUDHIR JAIN²

ABSTRACT

In theory, the porous zones in carbonates may be identified on reflection seismic data by changes in the rate of amplitude variation with increasing offsets in common-depth-point gathers, the amplitudes and/or wavelengths of appropriate reflections in normal-incidence (stacked) traces, and the velocities computed by amplitude inversion. To evaluate these processes, sonic and density logs were studied from two wells, one gas-producing and the other dry, for variations in amplitude vs offset, normal-incidence amplitude variations and amplitude inversion for velocity contrast. This study was extended to another well where porous zones were simulated for varying thickness and velocity contrast in a carbonate environment. For all synthetics, the amplitude variation with offset was insignificant, for practical offsets, relative to noise expected on prestack data, and this was confirmed by a set of real data. Ten-metre thick porous zones could be identified by small amplitude changes in the event corresponding to the top of the limestone and by velocity reduction in inverted sections. On real data, gas production could be identified as an amplitude increase in the Swan Hills reflector and as a distinct low-velocity zone on inversion. The dry well has a thin shale stringer in place of porosity with a similar effect on acoustic impedance as a gas zone, and this study did not find any way to separate them.

1. change in rate of amplitude variation with increasing offset in common-depth-point (CDP) gathers;
2. amplitude and/or wavelength changes in reflections from the vicinity of the top part of the reef;
3. changes in velocity computed by amplitude inversion of stacked traces.

In order to evaluate these three approaches, we conducted a synthetic study over two wells *A* and *B* within a few kilometres of each other in central Alberta. Well *A* has known production from an 18-m thick porous zone (average porosity 15 percent) in the Swan Hills Formation of the Beaverhill Lake Group (Figure 1) and well *B* has a thin shale stringer corresponding to porosity in well *A*. In an extension of this study, the sonic log from another well, *C*, also from central Alberta, was repeatedly altered to simulate various thickness and porosity parameters near the top of a carbonate formation overlain by clastic deposits. Normal-incidence and offset traces for source-receiver offsets up to 4600 m were computed. Normal-incidence traces were processed for velocity inversion using the process described by Jain and Wren (1977). This paper describes the result of these studies and discusses some real data examples which confirm the synthetic studies.

INTRODUCTION

While the detection of limestone reefs has been a popular subject in seismic literature (Agnich, 1956; Marr, 1971; Anderson et al., 1987, 1989), papers on the actual detection of porous zones are rare (Davis, 1980; Jain, 1986; Bower et al., 1987), although numerous studies have been undertaken by most exploration companies. Detection of porous zones is important because the existence of the reef does not by itself guarantee the existence of a sealed reservoir. Moreover, detection of the porous zone and its extent provides estimates of reservoir size and subsequent economic projections become more meaningful.

While a reef is identified on reflection seismic data by temporal changes and/or subtle amplitude changes in the key reflector, the existence of porosity may be indicated by any or all of the following:

AMPLITUDE-VERSUS-OFFSET (AVO) MODELS

Study of two sonic/density logs from wells *A* and *B*

The sonic and density logs were averaged for a 2-ms sample interval for gas well *A* and dry well *B*. Integrated logs and acoustic impedances from these wells are shown in Figure 2. Three sets of synthetic offset records were generated, two for well *A* and one from well *B* (Figure 3). Poisson's ratios were held constant at 0.28 for both wells. This value is appropriate for carbonates, too high for sands and a little too low for shales. The centre set shows the traces generated for well *A* with Poisson's ratio 0.28 for the porous zone in the carbonate. The left set was calculated for Poisson's ratio of 0.15 over an 18-m thick porous zone containing gas. The right set was computed for well *B* with

¹Presented at the C.S.E.G. National Convention, Calgary, Alberta, May 5, 1988. Manuscript received by the Editor September 1, 1988; revised manuscript received October 17, 1988.

²Commonwealth Geophysical Development Co., Ltd., 1701, 505 3rd Street S.W., Calgary, Alberta T2P 3E6

The authors acknowledge the assistance of Dan Petch and Allan Green in processing and of Deb Szoo and Jill Friesen in the preparation of the manuscript.

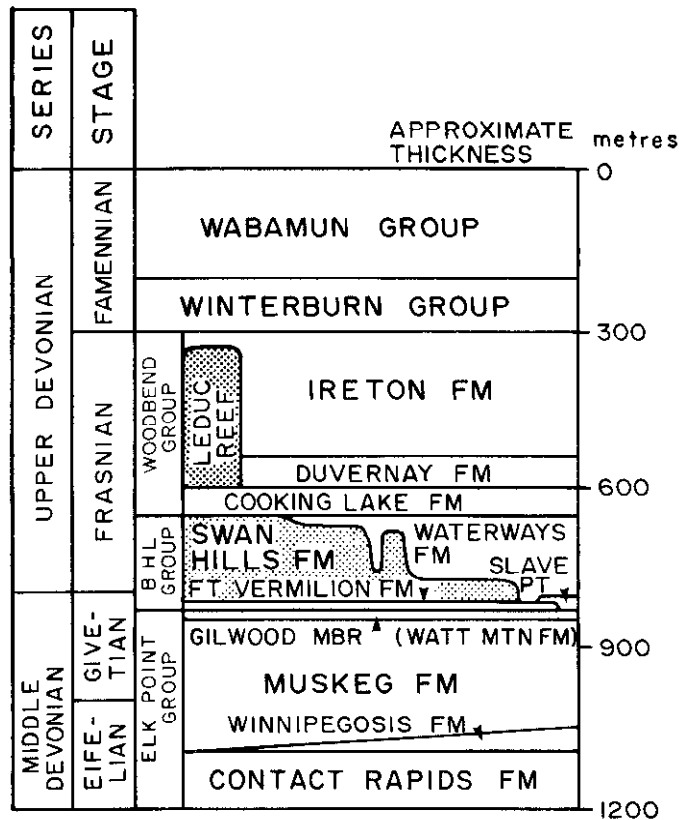


Fig. 1. Stratigraphic column of the Middle and Upper Devonian (after Anderson et al., 1989); BHL = Beaverhill Lake.

a Poisson's ratio of 0.28 in the expected porous zone. Zoeppritz's equations (Telford et al., 1976) were used to calculate reflected amplitudes for angles of incidence computed by ray tracing. Transmission and relative spherical-divergence losses were incorporated into the equations.

Synthetic traces were computed for a 24-trace spread with the first trace corresponding to zero offset and subsequent trace offsets increasing by 200 m. A zero-phase trapezoidal filter of passband 10/15-70/90 Hz was applied. This passband range is broader than normally observed in the western Canadian basin but was considered appropriate for this experiment in order to preserve resolution in the AVO study. The Swan Hills zone is indicated by the arrows in Figure 3. The colour bar relates to the amplitudes; red and orange represent negative numbers, green and blue the positive numbers. In all three synthetic records, amplitudes increase noticeably as offsets approach 4 km and the angle of incidence approaches the critical angle of 54 degrees. As expected, there is a small reduction in amplitude with offset for offsets up to 3 km for both wells when the Poisson's ratio is 0.28. When the Poisson's ratio is 0.15, the amplitudes increase marginally with offset. However, the relative amplitude changes are very small and will normally not be observed on real prestack data where the noise component is quite significant.

Alteration of sonic log C

Synthetic offset traces were generated from a sonic log from well C after integration at a 2-ms sample interval.

Densities were computed using an empirical velocity-density relationship given by Gardner et al. (1974) since the density log was not available. This approach is justified in our experience because, in general, velocities and densities behave predictably in carbonates even if they sometimes do not follow this particular empirical relationship exactly. Poisson's ratios were empirically computed from velocities and varied between 0.23 and 0.40 for clastics and 0.20 and 0.24 for carbonates. Synthetic traces were computed for a 24-trace spread as described above and displayed with a slightly different colour code (Figure 4). The expected porosity zone is shown by an arrow at approximately 1180 ms which is considerably shallower than in well A. Note that a weak trough on the normal-incidence trace declines slowly in amplitude up to a 2200-m offset. After this the amplitude of reflections increases dramatically due to critical reflection. Note that in the case of well C, the critical angle (38 degrees) is smaller than in wells A and B because of the sharp velocity increase at the clastics/limestone interface (at approximately 1.175 s). Figure 5 shows the same synthetic except that the zone from 1184 to 1190 ms (1780 to 1800 m) was altered to correspond to the gas reservoir with velocity 2000 m/s less than the velocity used in Figure 4 and with a Poisson's ratio of 0.15. The trough at 1184 ms has, indeed, a greater amplitude at all offsets, but amplitudes still decline with increasing offset, though at a lesser rate than in Figure 4. The arrival of totally reflected energy is approximately at the same offset in the two figures. This leads to the conclusion that, while amplitudes themselves may indicate the presence of gas-filled porosity, differences in amplitude variation with offset are too small to be observed for a 20-m thick porosity zone at a depth of 1780 m and with a Poisson's ratio of 0.15. These results are in agreement with those from wells A and B. Considering that most carbonate reservoirs in the western Canadian basin are deeper, thinner and less porous than this example and that the data before stack are contaminated by significant noise energy, the probability of observing porosity-related offset-amplitude anomalies is very small. Note that Jain (1987) used simplified Zoeppritz's equations given by Shuey (1985) to explain why anomalies in amplitude variations with offset are expected to be small except in rare cases of transparent reflectors.

Real data example

A plot of the amplitude coefficients (Jain, 1987) calculated from amplitudes of an actual data set in the Caroline area is shown in Figure 6. The field data were acquired for 15-fold stack with source-to-receiver offsets ranging from 300 to 3000 m. The zones of interest are the Leduc and Swan Hills at approximately 1675 ms and 1800 ms respectively. Positive coefficients (indicated in blue) denote amplitude increase with offset. Although one anomaly at 1675 ms corresponds to a 1-m thick zone of Leduc gas, other anomalies apparent at the Swan Hills did not prove to be gas-bearing. Over the entire section many anomalies

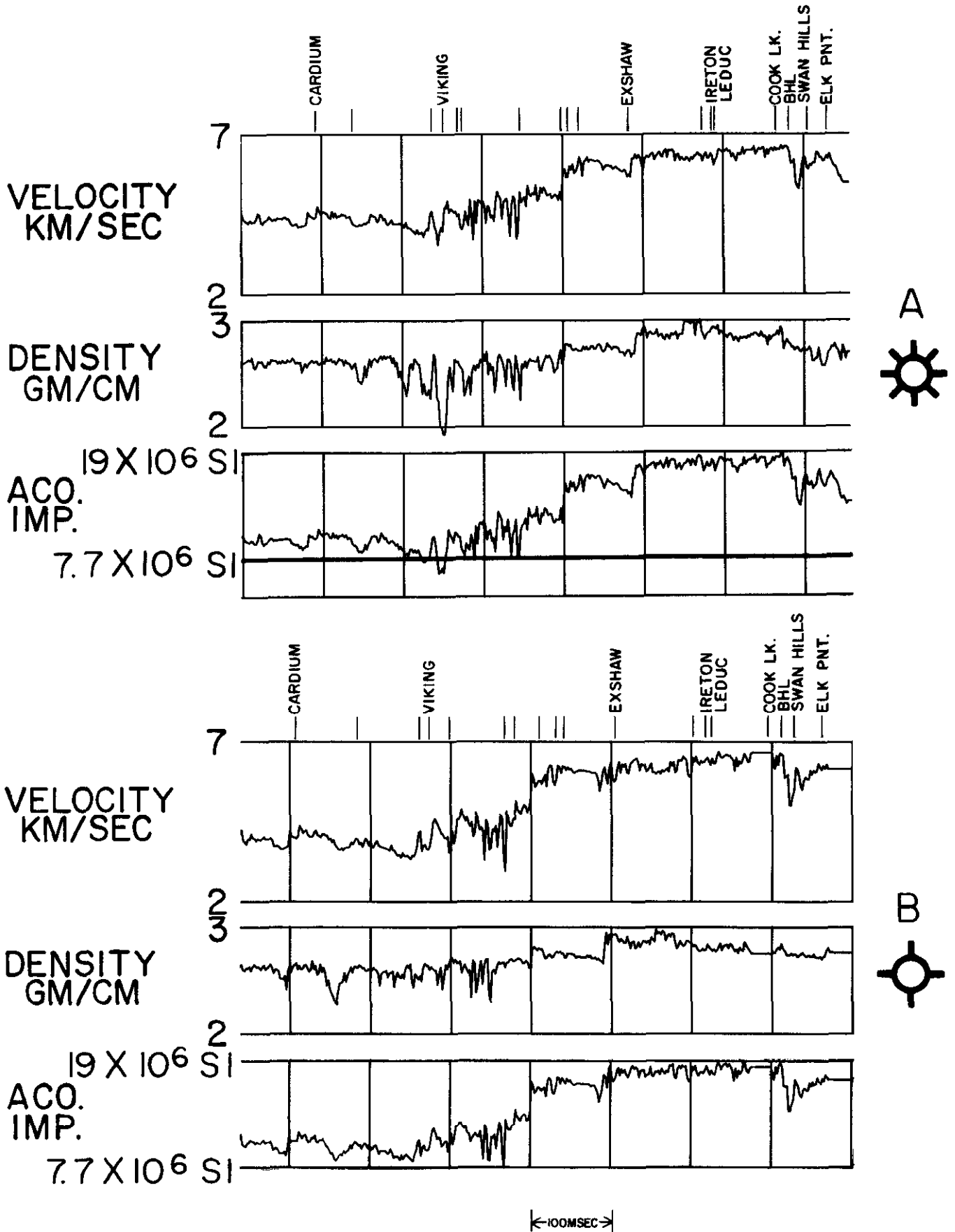


Fig. 2. Velocity, density and acoustic impedance from gas well A and abandoned well B.

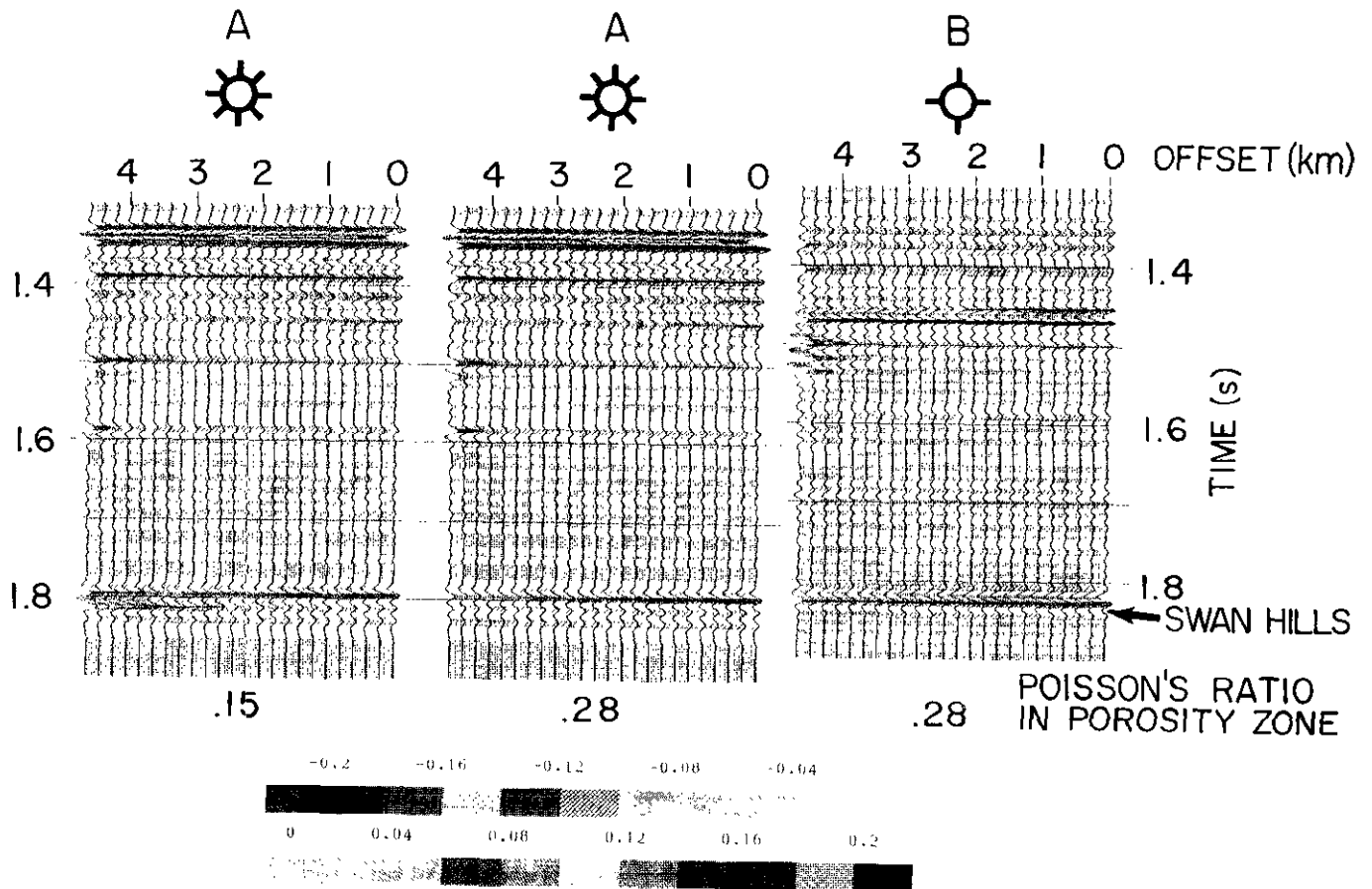


Fig. 3. Synthetic offset traces for offsets 0 to 4600 m for gas well A with Poisson's ratio = 0.15 and 0.28 for porous zones and for unproductive well B. Colours represent amplitude ranges indicated in the colour bar.

suggesting gas reservoirs are present, which is clearly not a realistic situation. These positive amplitude coefficients are most probably caused by noise present in the data. Figure 7 shows eight normal-moveout-corrected CDP gathers across

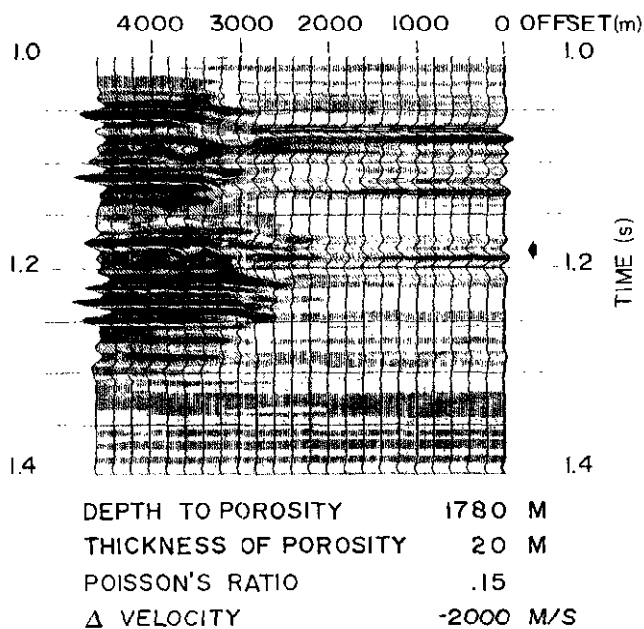


Fig. 4. Synthetic offset traces for offsets 0 to 4600 m for well C; same colour code as in Figure 3.

the gas well after numerous attempts at signal/noise ratio enhancement including two-dimensional filtering and 4:1 common-offset stack. Changes in amplitude and character within CDP gathers and from one gather to the next indicate poor signal/noise ratio and explain the random nature of the amplitude coefficients in Figure 6.

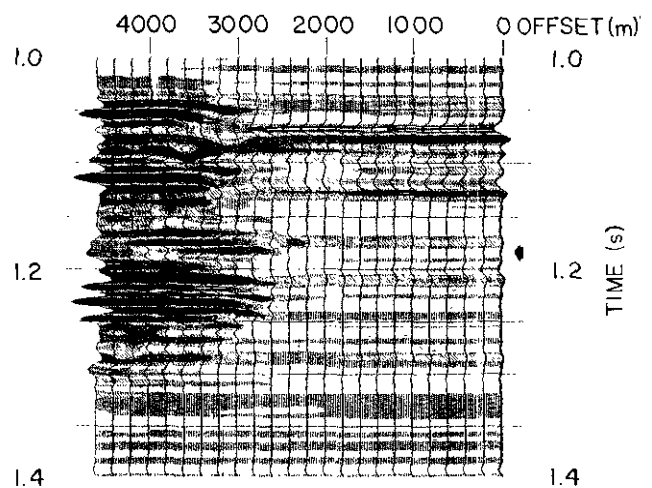


Fig. 5. Synthetic offset traces corresponding to those in Figure 4 except that a 20-m thick porous zone with porosity = 0.15 has been introduced at a depth of 1780 m as shown by arrow; same colour codes as in Figures 3 and 4.

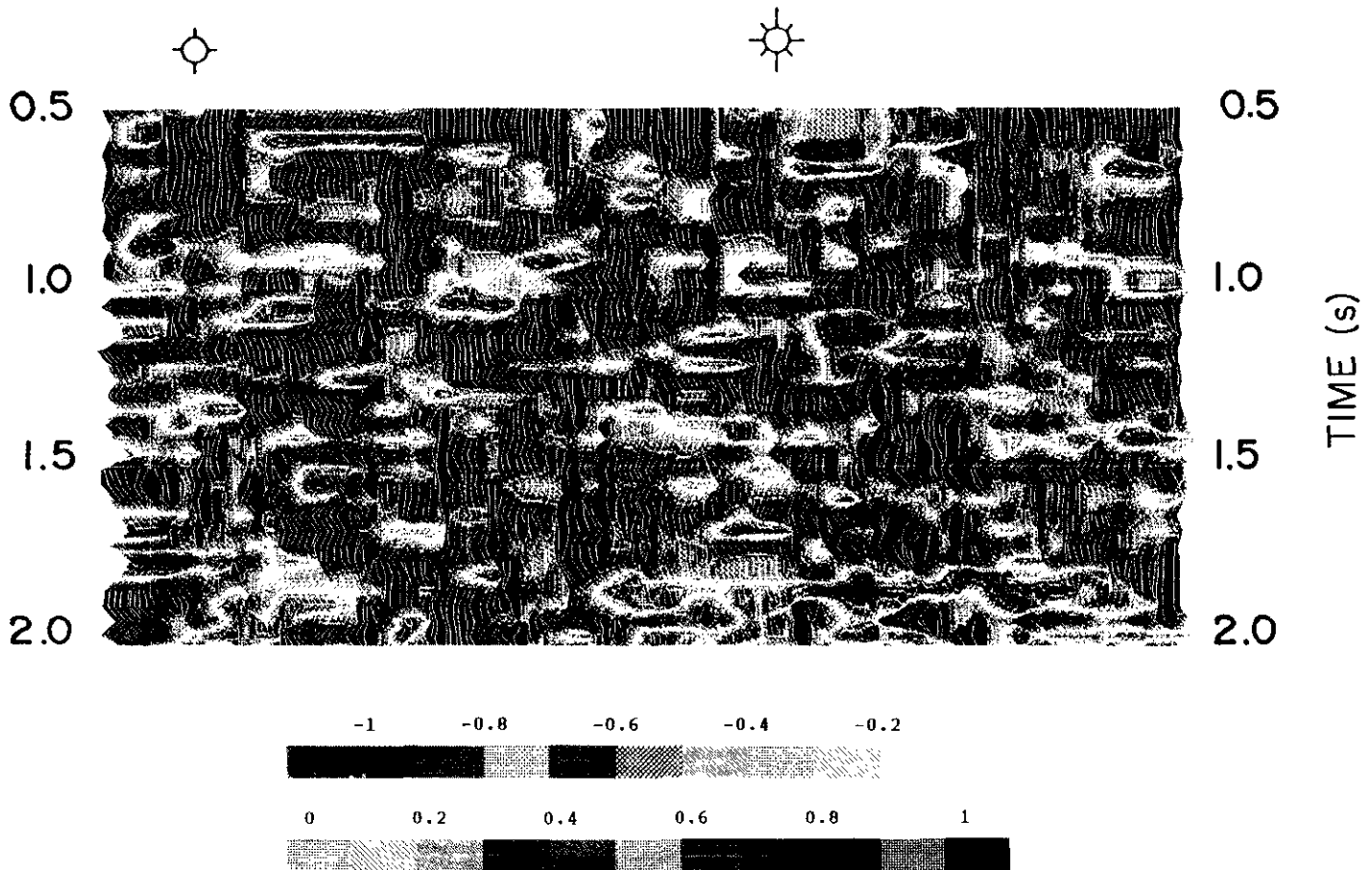


Fig. 6. Amplitude coefficients from a set of CDP gathers at Caroline, Alberta. Positive values in blue denote an increase in amplitude with offset.

AMPLITUDE OF STACKED TRACES

When static and dynamic corrections and deconvolution are handled properly, the stacking process improves the signal/noise ratio of recorded data to such an extent that it becomes realistic to analyse amplitude and frequency characteristics of particular reflections (Sangree and Widmier, 1979; Taner et al., 1979). Generally, the sonic logs are modelled with expected changes and the resulting synthetic traces are examined to determine the characteristics of carbonate porosity (or any other feature) to be identified on the stacked traces (Edwards, 1988).

Wells A and B

The velocity, density and acoustic-impedance plots for the wells A and B are shown in Figure 2. Note that well B has a lower velocity in the Swan Hills due to a shale stringer while well A has the lower density. As a result, the acoustic impedance in the two wells is very similar in the critical zone. Figure 8 shows, in both polarities, the synthetic traces computed from the acoustic impedances in the two wells. The wavelet was zero-phase with the trapezoidal passband 10/15-45/55 Hz, which is appropriate for most seismic data in the western Canadian basin at approximately 1.5 to 2.0 s of two-way traveltime. Gas well A and abandoned well B have almost identical peak-trough

amplitudes for the Beaverhill Lake marker but show differences in character. For example, a low-velocity zone associated with the Cooking Lake Formation in well B causes tightening of the peak above the main trough on the normal-polarity synthetic. Also, the leg following the peak is broader on the gas well because of the broadening of a low acoustic-impedance zone in the Swan Hills Formation. Whether any of these features is associated with production cannot be established with any certainty.

Modification of sonic log from well C

Well C discussed earlier was altered in the zone near the top of the carbonate section as shown in Figure 9. The thickness of the porous zone was either 10 m or 20 m and the velocity contrast due to porosity was 500 m/s (porosity 9 percent), 1000 m/s (porosity 18 percent), or 2000 m/s (porosity 35 percent). Density was computed using the empirical velocity-density relationship given by Gardner et al. (1974).

Figure 10 shows the amplitude of the synthetic traces computed with the zero-phase wavelet of trapezoidal passband 10/15-70/90 Hz. Synthetic traces are plotted in sets of four traces for each alteration, the unaltered sonic being represented by the top four traces. The synthetic traces show small differences in amplitudes for a velocity change

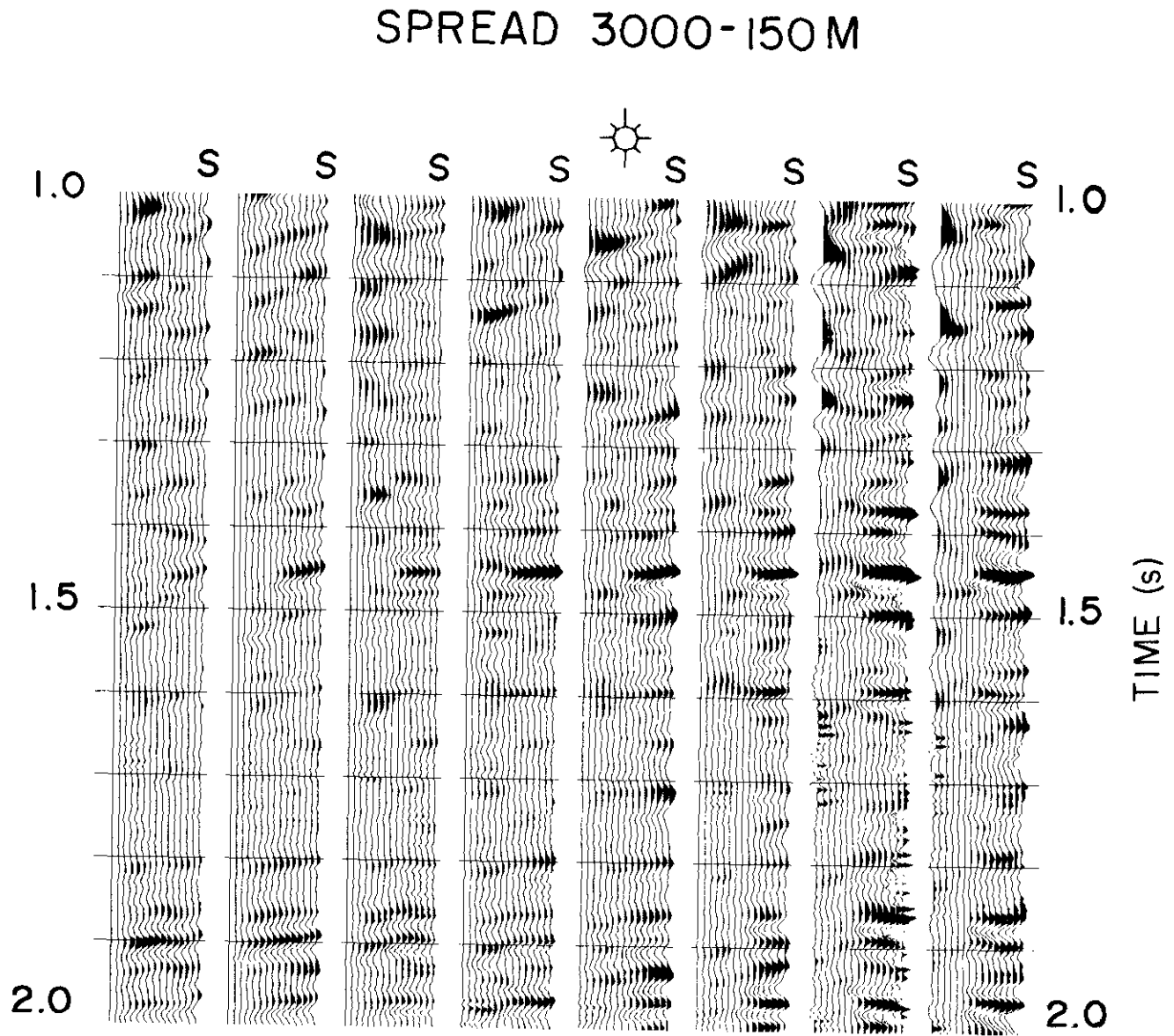


Fig. 7. Examples of normal-moveout corrected CDP gathers after signal/noise ratio enhancement for the spread 0-150-3000 m.

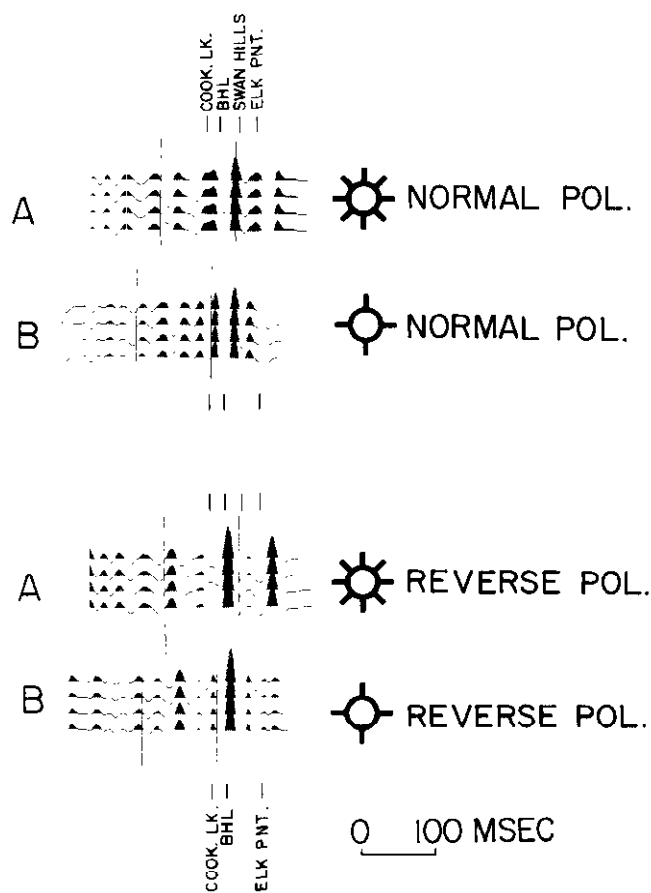


Fig. 8. Synthetic traces, generated from acoustic impedances in Figure 2, in both polarities.

of 1000 m/s for both 10-m and 20-m thick porosity zones. When the velocity contrast is 2000 m/s, the amplitude of the trough increases and the event broadens for both thicknesses. Therefore, highly porous carbonate zones with a thickness of 10 m or more can be identified by amplitude changes on stack sections. These changes indicate velocity contrast, not necessarily porosity. As shown above in wells *A* and *B*, a thin shale stringer causes the same amplitude anomaly as a porous limestone zone when acoustic-impedance contrasts are similar.

Real data

Figure 11 shows a reversed-polarity 15-fold stack section from the Caroline area in central Alberta. One gas producer (well *A*) and a dry well are located on the profile. The Swan Hills reflector broadens and shows increased amplitude below the gas well and is quite weak below the dry well. However, the amplitude declines only slightly to the left of the gas well, and the margin of the gas zone on this side is not evident. This is possibly due to interference from the second leg of the Beaverhill Lake reflector.

AMPLITUDE INVERSION

The computation of acoustic impedance from seismic reflection data (Delas et al., 1970; Jain and Wren, 1977; Lindseth, 1979), often called amplitude inversion (or sim-

ply inversion), is now an established technique for exploration in a variety of lithologic environments (Jain, 1986). Although acoustic impedance is computed from amplitudes of normal-incidence traces, results are normally presented in terms of velocities based on some empirical relationship between velocity and density. Inversion is often helpful in two ways. The process of derivation of reflectivities from stacked traces enhances the resolution, and the velocity computation from reflectivities increases the dynamic range of displays so that very small changes can be observed on an inversion display. Colour displays of velocities enhance visual appeal although they do not improve resolution as is sometimes believed.

The inversion process followed in this study was described by Jain and Wren (1977). In brief, a statistical wavelet is computed from each seismic trace over a window of approximately one-second duration that includes the zone of interest. The operator is designed to reduce this wavelet to a spike and is applied to the trace. This operation reduces the trace to a series of spikes which are equivalent to a scaled version of reflectivities encountered by the propagating wavelet. The spikes do not duplicate those from a sonic log because seismic data is band-limited. The spikes computed from this data are spaced 4 to 6 ms apart to show the lack of high frequencies in seismic data. Also, the velocities computed from these reflectivities alone do not have low-frequency components (gradual increase and large steps) often noted on sonic logs. In order to minimize errors in velocity computation, the low-frequency component is added to the computed reflectivities before computing final velocities. This low-frequency component is computed either from an analysis of normal-moveout velocities or from a study of sonic logs in the area.

Wells *A* and *B*

The velocities, densities and acoustic impedances (Figure 2) and the corresponding synthetic traces (Figure 8) were discussed earlier. Although the impedances in the two logs show a great deal of similarity, there are small differences in detail which show up as small differences in the synthetic seismograms. The synthetic traces were inverted using the wavelets extracted from these traces and the low-frequency velocity component (a simple linear ramp function) suggested by the wells. The computed velocities are shown in Figure 12 as sets of four traces. The impedances are reproduced from Figure 2 to facilitate comparison. The following observations are of interest in Swan Hills porosity exploration:

1. Both wells show that the impedance is less in the Swan Hills Formation than in the Cooking Lake Formation. The inversion velocities do not show this due to the lack of low frequencies in the seismic data.
2. Well *B* shows a relative decline in inversion velocity near the top of the Beaverhill Lake. This is due to reduction in the impedance of the Cooking Lake Formation which caused the tightening of the peak referred to earlier.

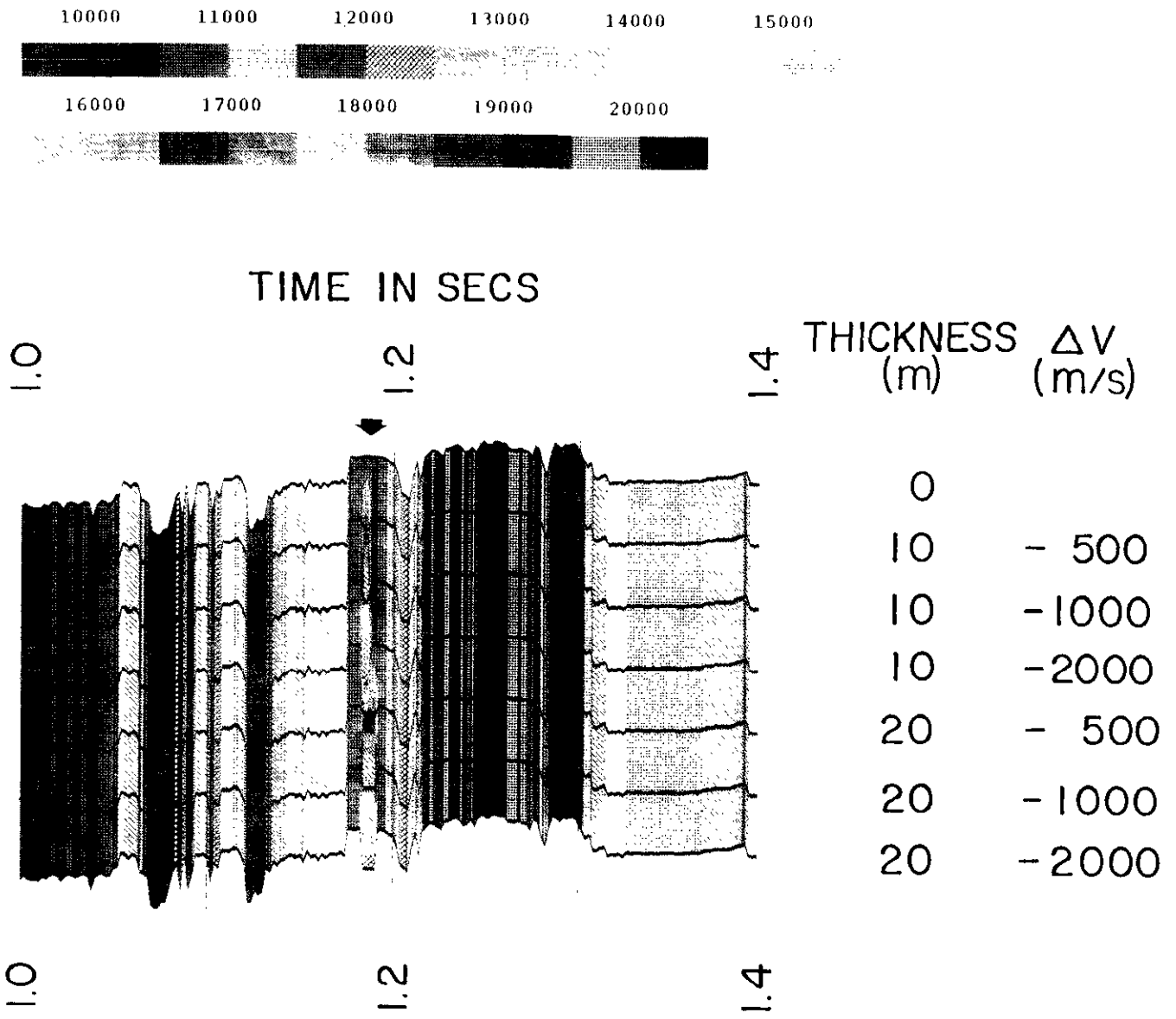


Fig. 9. Alterations applied to the sonic log from well C. Colours represent interval velocities in ft/s (1ft/s ≈ 0.3 m/s).

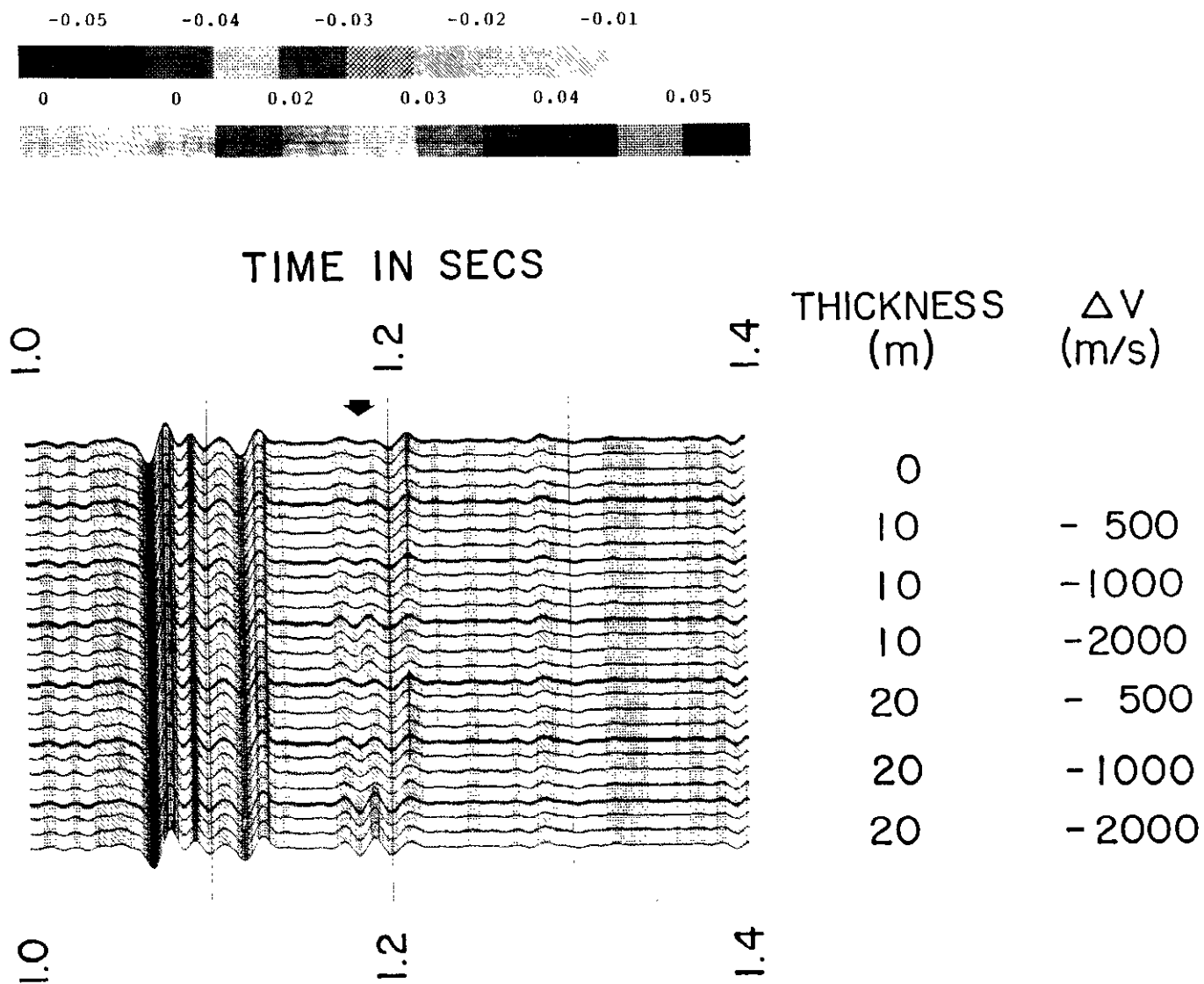


Fig. 10. Synthetic traces computed from well C after the alterations shown in Figure 9. Colours represent amplitude.

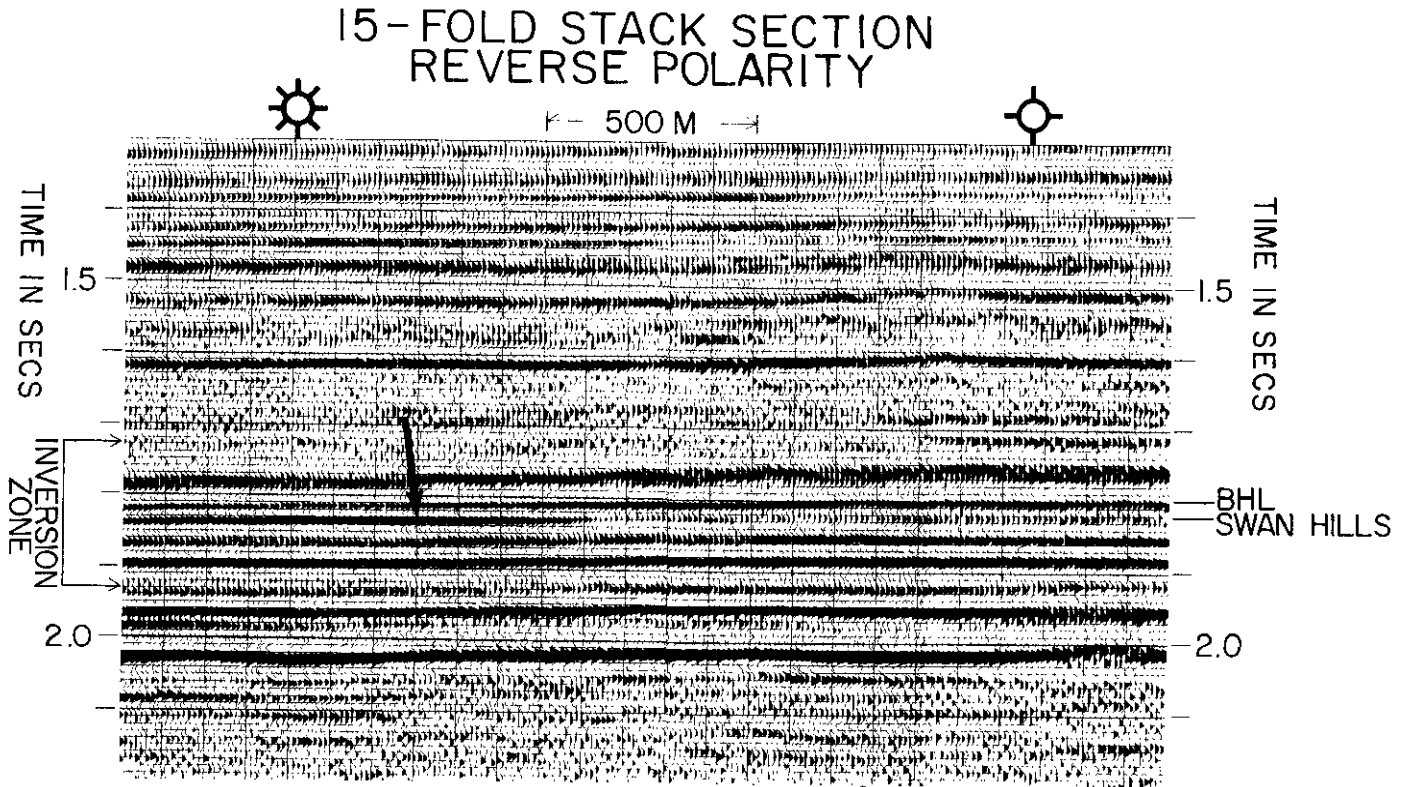


Fig. 11. A stacked section from the Caroline area of Alberta with one gas-producing and one dry well. The thick arrow indicates the reflector corresponding to the gas zone.

3. The impedance peak at the base of the Swan Hills porosity (indicated by an arrow in Figure 12) is more prominent in gas well A than in well B. This is shown in inversion traces as a 6-ms (approximately 18-m) thick step in well A just before reaching the peak velocity below the Beaverhill Lake shale. In well B, inversion traces reach higher velocity at the base of the Beaverhill Lake and are practically flat for 16 ms (approximately 50 m). This observation is similar to that of Bower et al. (1987) at Judy Creek, Alberta.

Studies from more wells are needed to establish whether any or all of these features are associated with production. Whether these features can be observed in these forms on real data which have short- and long-period multiples and other noise trains in varying proportion is also open to question.

Inversion of synthetic models from well C

The synthetic traces (Figure 10) computed by alterations of well C (Figure 9) were "inverted" and the results are shown in Figure 13. A 10-m thick porosity zone is not apparent when the velocity contrast is 500 m/s. This zone becomes visible (thickening light blue) when the velocity contrast is 1000 m/s and stands out as a distinct zone at 2000 m/s. A 20-m thick porosity zone is visible when the contrast is 500 m/s (thick light blue). It becomes more pronounced when the contrast is 1000 m/s and is a thick and clear trough when the contrast is 2000 m/s. Note that it is possible to deduce the thickness of the zone from the width of the lowest contour only when the contrast in velocities

is 2000 m/s. In computing velocities for thin zones with smaller contrast, the resolution of seismic data does not allow the estimation of both thickness and velocity contrast (thus porosity) and only the combined effect of the two can be estimated (Jain, 1986). An unfortunate implication of this observation is that a thin shale stringer with large velocity reduction can appear as a porosity zone of reason-

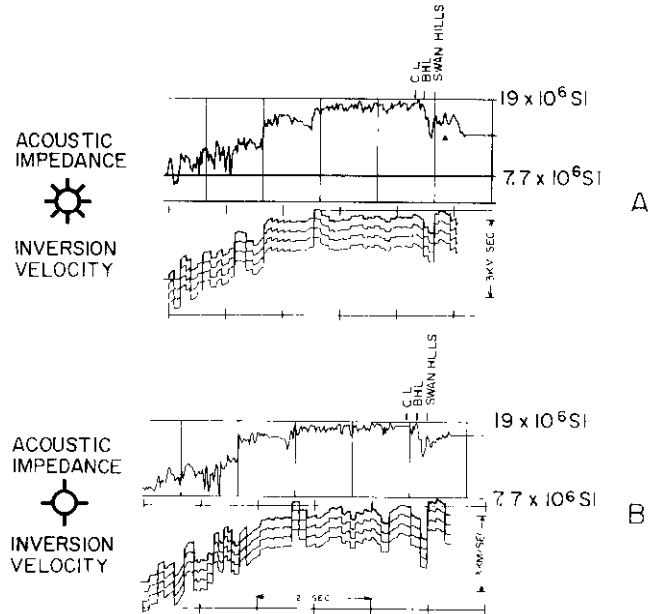


Fig. 12. Original acoustic impedance and the inversion velocities computed from synthetic traces (repeated four times) for producer A and abandoned well B.

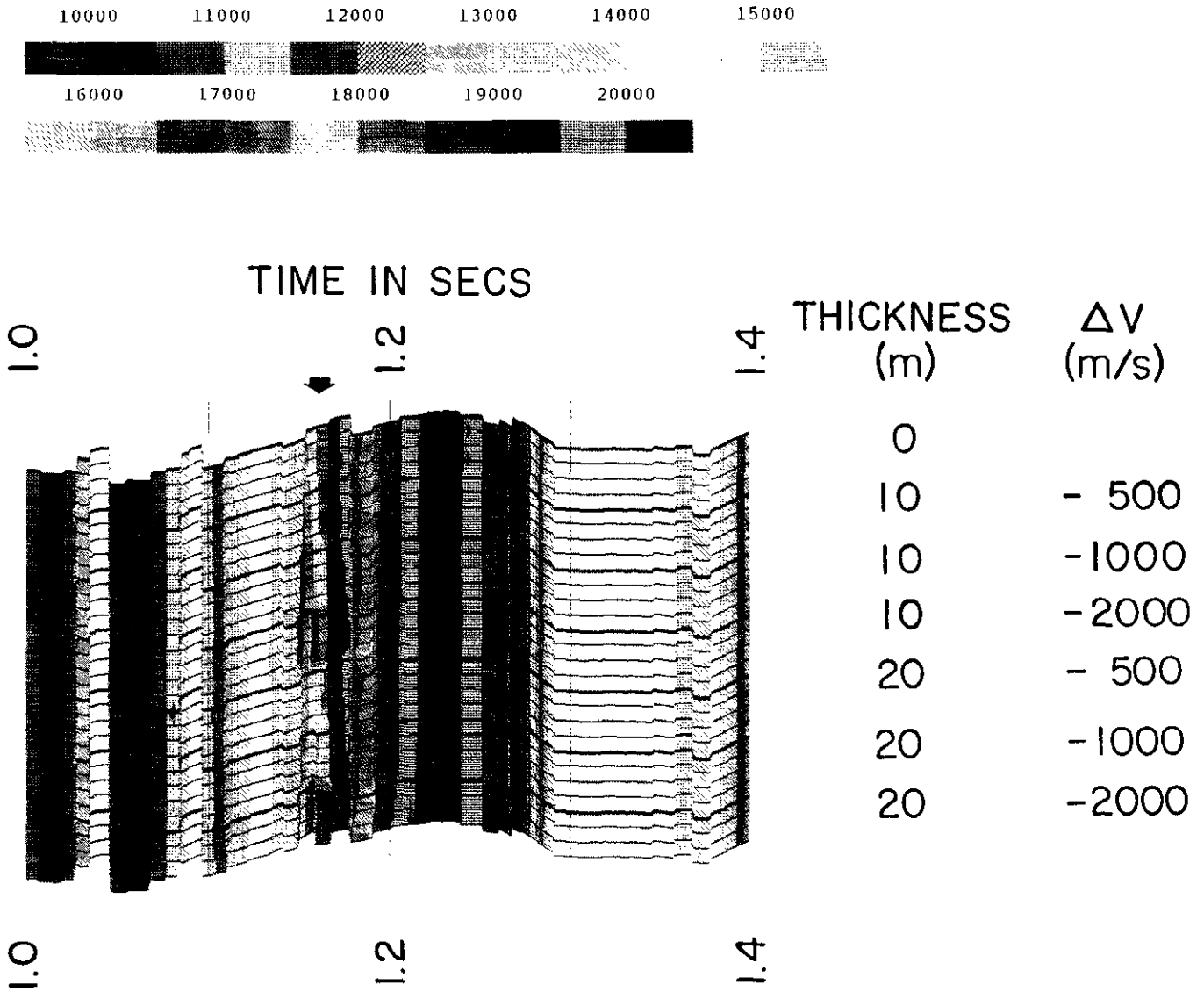


Fig. 13. Inversion of synthetic traces in Figure 10. Colours represent interval velocity in ft/s (1 ft/s = 0.3 m/s). The arrow points to the peak referred to in the text.

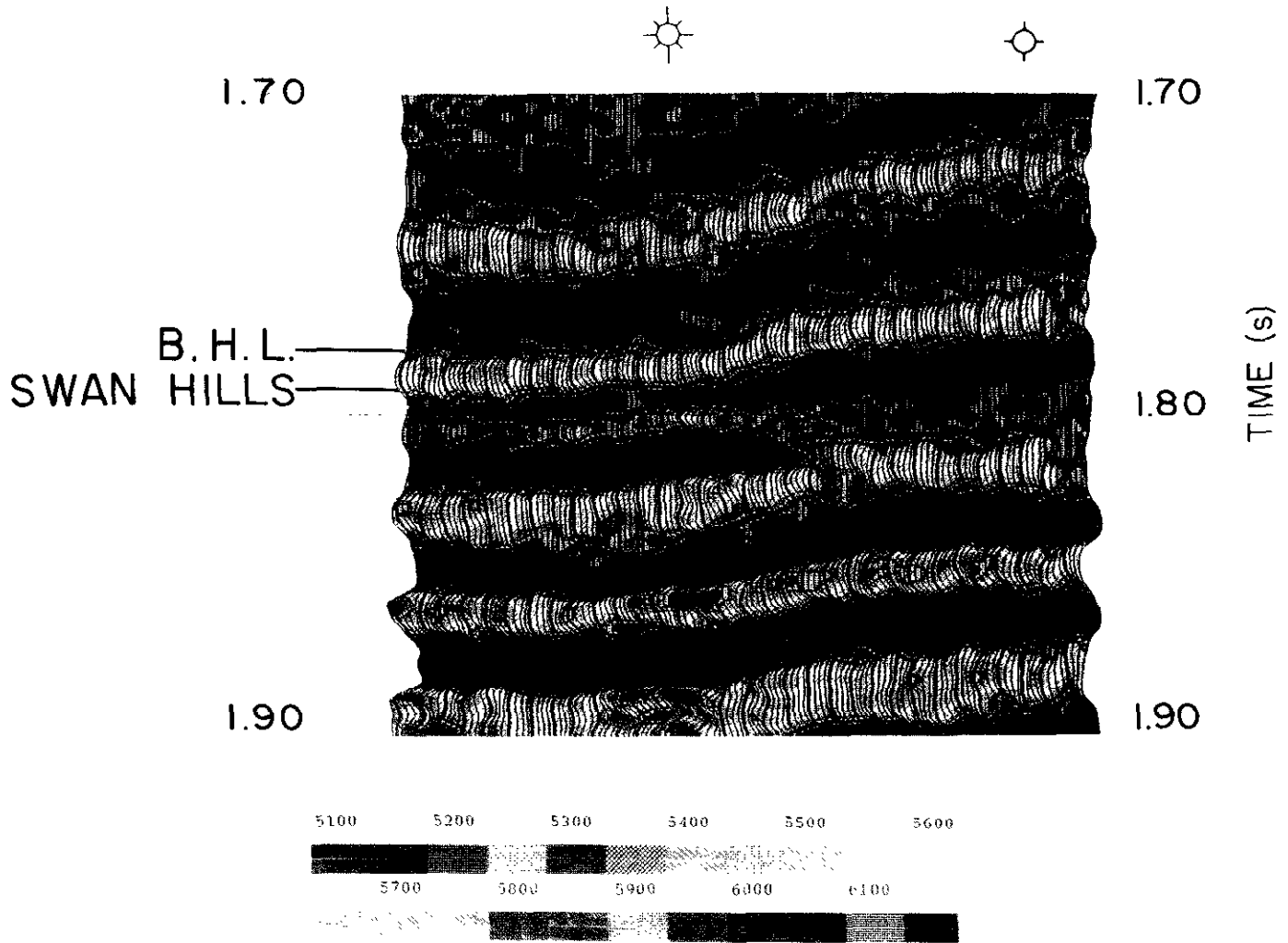


Fig. 14. Inversion of the profile shown in Figure 11. Colours represent interval velocity in m/s as shown in the colour code.

able thickness. This emphasizes the importance of the understanding of local geology in order to define the carbonate bank edge and to avoid drilling a shale stringer in the basin.

Inversion of real data

Figure 14 shows an example of seismic inversion of the stacked section shown in Figure 11 at an enlarged temporal scale. Time shift on inversion is due to the compensation for wavelet delay in stacked sections. Arrows in Figure 11 indicate the time zone shown in Figure 14. The porous reservoir under the gas well is shown as a blue elongated lens terminating abruptly at each end. There is no velocity anomaly at this level below the dry well. While the velocity low corresponds to the gas well, it may be noted that a thin shale lens at the same level would have produced the same effect. However, the dry hole on the right would not have been drilled for Swan Hills porosity after inversion.

CONCLUSIONS

Synthetic traces from sonic and density logs of one gas producer and one abandoned well, synthetic traces from

modifications of a sonic log from another well, and sets of real data with respect to amplitude variations with offset, normal-incidence (stacked trace) amplitudes and amplitude inversion were analyzed. It was found that the seismic data are only partially helpful in locating porosity in carbonates. Velocity reductions due to porosity could be identified as small amplitude changes on stacked sections and as velocity reductions on inversion sections. The AVO anomalies were very small relative to the noise generally present on prestack data. Therefore, gas-bearing zones can be distinguished from shale stringers on seismic data only with an adequate understanding of local geology.

REFERENCES

Agnich, F.J., 1956, Geophysical exploration for limestone reefs: *Geophysical Case Histories* 2, 72-86.
 Anderson, N.L. and Brown, R.J., 1987, The seismic signatures of some western Canadian Devonian reefs: *J. Can. Soc. Expl. Geophys.* 23, 1-26.
 ..., Hinds, R.C. and Hills, L.V., 1989, Seismic signature of a Swan Hills (Frasnian) reef reservoir, Snipe Lake, Alberta: *Geophysics* 54, in press.

- Bower, P., Boyd, J. and Jain, S., 1987, Locating Swan Hills porosity at Judy Creek using seismic inversion: *J. Can. Soc. Expl. Geophys.* **23**, 37-45.
- Davis, T.L., 1980, Application of reflection seismology to Mississippian carbonate porosity and direct hydrocarbon detection: *J. Can. Soc. Expl. Geophys.* **16**, 19-25.
- Delas, C., Beauchamp, J.B., de Lombares, G., Fourmann, J.M. and Postic, A., 1970, An example of practical velocity determinations from seismic traces: Presented at the 32nd Mtg., Eur. Assn. Expl. Geophys., Edinburgh.
- Edwards, S., 1988, Uses and abuses of seismic modeling, *Leading Edge* **7**, 4, 42-46.
- Gardner, G.H.F., Gardner, L.W. and Gregory A.R., 1974, Formation velocity and density — The diagnostic basics for stratigraphic traps: *Geophysics* **39**, 770-780.
- Jain, S., 1986, Suitable environments for inversion techniques: A model study: *J. Can. Soc. Expl. Geophys.* **22**, 7-16.
- _____, 1987, Amplitude-vs-offset analysis: A review with reference to application in western Canada: *J. Can. Soc. Expl. Geophys.* **23**, 27-36.
- _____, and Wren, A.E., 1977, The application of optimal wavelets in seismic inversion: *J. Can. Soc. Expl. Geophys.* **13**, 3-14.
- Lindseth, R.O., 1979, Synthetic sonic logs, a process for stratigraphic interpretation: *Geophysics* **44**, 3-26.
- Marr, J.D., 1971, Seismic stratigraphic exploration — Part II: *Geophysics* **36**, 533-553.
- Sangree, J.B. and Widmier, J.M., 1979, Interpretation of depositional facies from seismic data: *Geophysics* **44**, 131-160.
- Shuey, R.T., 1985, A simplification of the Zoeppritz equations: *Geophysics* **50**, 609-614.
- Taner, M.T., Koehler, F. and Sheriff, R.E., 1979, Complex seismic trace analysis: *Geophysics* **44**, 1041-1063.
- Telford, W.M., Geldart, L.P., Sheriff, R.E. and Keys, D.A., 1976, *Applied geophysics*: Cambridge Univ. Press.